Lawrence Berkeley National Laboratory
LBL Publications

Title
{sup 18}O composition of CO{sub 2} and H{sub 2}O ecosystem pools and fluxes in a tallgrass prairie: Simulations and comparisons to measurements

Permalink
https://escholarship.org/uc/item/3b32p275

Authors
Riley, William J.
Still, Christopher J.
Helliker, Brent R.
et al.

Publication Date
2002-11-01

^{18}O composition of CO_2 and H_2O ecosystem pools and fluxes in a tallgrass prairie: Simulations and comparisons to measurements

W I L L I A M   J .   R I L E Y*, C H R I S T O P H E R   J .   S T I L L †, B R E N T   R .   H E L L I K E R ‡, M I G U E L   R I B A S - C A R B O §, and J O S E P H   A .   B E R R Y ‡

*Earth Sciences Division, Lawrence Berkeley National Laboratory, Bldg 90-1106, 1 Cyclotron Road, Berkeley, CA 94720, USA, †Department of Geography, 3611 Ellison Hall, University of California, Santa Barbara, CA 93106, USA, ‡Department of Global Ecology, Carnegie Institution of Washington, 260 Panama Street, Stanford, CA 94305, USA, §Departamento de Biologia, Area de Fisiologia Vegetal, Universitat de les Illes Balears, Ctra de Valldemossa, km 7.5, 07071 Illes Balears, Spain

Abstract

In this paper we describe measurements and modeling of ^{18}O in CO_2 and H_2O pools and fluxes at a tallgrass prairie site in Oklahoma. We present measurements of the $\delta^{18}O$ value of leaf water, depth-resolved soil water, atmospheric water vapor, and Keeling plot $\delta^{18}O$ intercepts for net soil-surface CO_2 and ecosystem CO_2 and H_2O fluxes during three periods of the 2000 growing season. Daytime discrimination against $C^{18}OO$, as calculated from measured above-canopy CO_2 and $\delta^{18}O$ gradients, is also presented. To interpret the isotope measurements, we applied an integrated land-surface and isotope model (ISOLSM) that simulates ecosystem $H_2^{18}O$ and $C^{18}OO$ stocks and fluxes. ISOLSM accurately predicted the measured isotopic composition of ecosystem water pools and the $\delta^{18}O$ value of net ecosystem CO_2 and H_2O fluxes. Simulations indicate that incomplete equilibration between CO_2 and H_2O within C_4 plant leaves can have a substantial impact on ecosystem discrimination. Diurnal variations in the $\delta^{18}O$ value of above-canopy vapor had a small impact on the predicted $\delta^{18}O$ value of ecosystem water pools, although sustained differences had a large impact. Diurnal variations in the $\delta^{18}O$ value of above-canopy CO_2 substantially affected the predicted ecosystem discrimination. Leaves dominate the ecosystem ^{18}O-isoflux in CO_2 during the growing season, while the soil contribution is relatively small and less variable. However, interpreting daytime measurements of ecosystem $C^{18}OO$ fluxes requires accurate predictions of both soil and leaf ^{18}O-isofluxes.

Nomenclature

C_i = leaf internal CO_2 concentration ($\mu mol\,m^{-3}$)

C_H, C_L = CO_2 concentrations at the high and low sampling points ($\mu mol\,m^{-3}$)

F_{al}, F_{la} = CO_2 fluxes into and out of the leaf ($\mu mol\,m^{-2}\,s^{-1}$)

F_g, F_{sm}, F_s = growth, stem, and net soil-surface CO_2 fluxes ($\mu mol\,m^{-2}\,s^{-1}$)

I = ecosystem ^{18}O-isoflux ($\mu mol\,m^{-2}\,s^{-1}\,‰$)

R_a, R_c, R_e, R_{eq} = CO_2 ^{18}O isotopic ratios in the atmosphere, chloroplast, net ecosystem flux, and in equilibrium with leaf water

z_0 = e-folding depth for soil CO_2 source (m)

δ_a, δ_e, δ_l, δ_H, δ_L, δ_{nl}, δ_{sw}, δ_s = $\delta^{18}O$ values of atmospheric CO_2, net ecosystem CO_2 flux, leaf water; CO_2 at the high sampling point, CO_2 at the low sampling point, net leaf CO_2 flux, stem respiration CO_2 flux, and soil CO_2 flux (‰)

Δ_c = difference in $\delta^{18}O$ values of chloroplast and atmospheric CO_2 (‰)

Δ_{eq} = difference in $\delta^{18}O$ values of equilibrium chloroplast and atmospheric CO_2 (‰)

Correspondence: William J. Riley, fax 510 486 7070,
e-mail: wjriley@lbl.gov

$\Delta_L^{18}, \Delta_s^{18}, \Delta_e^{18} =$ net discrimination against $C^{18}OO$ from leaves, soil, and ecosystem (‰)
$\Theta_{eq} =$ disequilibrium between CO_2 and leaf water

Introduction

Terrestrial ecosystem carbon fluxes dominate large-scale spatial and temporal variations in the $\delta^{18}O$ value of atmospheric CO_2, δ_a (‰). Ocean gas exchange, biomass and fossil fuel burning, and stratospheric reactions also impact δ_a, although their influence is much smaller (Francey & Tans, 1987; Farquhar *et al.*, 1993; Ciais *et al.*, 1997a; Peylin *et al.*, 1999). At the global scale, a simple mass balance can be used to estimate the relative impact of these fluxes. The net ocean exchange, fossil fuel and biomass burning, and stratospheric fluxes are each less than $150 \, \mathrm{Pg \, C \, yr^{-1}}$‰, while the photosynthetic and soil respiratory fluxes are each on the order of $1000 \, \mathrm{Pg \, C \, yr^{-1}}$‰ (Tans, 1980; Farquhar *et al.*, 1993). Using a global network of flask data, Francey & Tans (1987) inferred that terrestrial carbon fluxes interacting with soil and leaf water drive the large (~ 1.5‰) observed interhemispheric gradient in δ_a. Simultaneously, Friedli *et al.* (1987) showed that terrestrial fluxes strongly influence measured variations in δ_a above Switzerland.

Experimental and theoretical advances in our understanding of respiratory and photosynthetic influences on δ_a followed these studies. In both respiration and photosynthesis, the exchange of oxygen isotopes between water and dissolved CO_2 imparts the $\delta^{18}O$ value of water to the CO_2 molecules. Hesterburg & Siegenthaler (1991) first investigated the interactions of soil CO_2 with soil water and developed a model to predict the $\delta^{18}O$ value of soil-respired CO_2. Tans (1998) expanded on this model to incorporate the influence of 'abiotic' or 'invasion' fluxes and developed analytical solutions for the $\delta^{18}O$ value of soil-gas CO_2 and surface CO_2 fluxes for a range of environmental conditions. Miller *et al.* (1999) performed a series of detailed measurements to quantify the effective kinetic fractionation of CO_2 diffusion out of the soil and demonstrated the importance of the invasion flux in soil chamber measurements. By applying the analytical solutions of Tans (1998), Stern *et al.* (2001) estimated the importance of abiotic CO_2 exchange between the atmosphere and soil for a variety of ecosystems. To quantify leaf $C^{18}OO$ exchanges, Farquhar & Lloyd (1993) developed equations describing interactions between leaf CO_2 fluxes and ^{18}O in leaf water. Leaf $C^{18}OO$ exchanges are dominated by the influx of CO_2 molecules into leaves, isotopic exchange with leaf water, and 'retrodiffusion' (i.e., molecules leaving the leaf without being fixed by photosynthesis, but having a different $\delta^{18}O$ value than when they entered).

Some of these results have been incorporated in global modeling studies of surface $C^{18}OO$ fluxes and δ_a. In the first such study, Farquhar *et al.* (1993) confirmed the importance of photosynthesis and respiration on δ_a. Ciais *et al.* (1997a, b) modeled net ecosystem $C^{18}OO$ fluxes and coupled them to a 3-D tracer-transport model to examine seasonal and latitudinal variations in δ_a. Using the same modeling framework, Peylin *et al.* (1999) explored the influence of specific geographic regions on temporal and latitudinal variations in δ_a. They argued that seasonal variations in northern hemisphere δ_a are dominated by carbon exchanges in the Siberian taiga region, where soil and leaf water are strongly depleted in ^{18}O. Despite these modeling advances, a number of uncertainties remain, including the large interannual variability and apparent downward trend in global measurements of δ_a (Gillon & Yakir, 2001; Stern *et al.*, 2001). Furthermore, the models of ecosystem $C^{18}OO$ fluxes used in these global-scale studies have not been adequately tested at the site level.

Several ecosystem-scale studies have reported using measurements of ^{18}O in H_2O and CO_2 to better understand controls on the $\delta^{18}O$ value of CO_2 exchanged with the atmosphere or to partition measured net CO_2 fluxes into gross fluxes (for reviews, see Yakir & Sternberg, 2000; Dawson *et al.*, 2002). Yakir & Wang (1996) used simultaneous measurements of ^{18}O and ^{13}C to partition net CO_2 fluxes between soil and plant components in several crop fields. Flanagan *et al.* (1995) described measurements of ^{18}O in water pools and CO_2 at two heights in a pine forest canopy. They reported that predictions from a mixing model that included the various ecosystem CO_2 sources were consistent with observed diurnal variations in $C^{18}OO$ concentrations within the canopy. Using discrimination calculations based on measurements of ^{18}O in soil, stem, and leaf water, Flanagan *et al.* (1997) estimated that mid-day discrimination against $C^{18}OO$ during photosynthesis was similar among the three boreal forest types, but that CO_2 released during soil respiration was less depleted than expected due to interactions with an extensive moss layer. In a tropical forest site, Harwood *et al.* (1998) reported leaf-level measurements of the

$\delta^{18}O$ value of CO_2 fluxes and their relationship to vapor pressure deficits and stomatal conductance. Harwood *et al.* (1999) used Keeling plot analysis in a UK forest site to demonstrate that heterogeneity in ecosystem water pools likely accounted for variations in the $\delta^{18}O$ value of CO_2 fluxes. Keeling plots and measurements of ^{18}O in ecosystem water pools have also been used to quantify soil and leaf contributions to the net ecosystem latent heat flux (Wang & Yakir, 2000).

The studies mentioned above were conducted in forest and agricultural ecosystems; much less information exists on ^{18}O exchanges in H_2O and CO_2 in grasslands, which cover close to 25% of the earth's land surface. Several recent studies indicate that $C^{18}OO$ exchanges may be more complicated than originally thought, particularly in C_4 grasslands. For example, incomplete isotopic equilibration (termed disequilibrium, Θ_{eq}) between CO_2 and leaf water due to low carbonic anhydrase (CA) enzyme activity may be common in most grasses (Gillon & Yakir, 2000, 2001). In this notation, Θ_{eq} varies between 0 and 1, and $\Theta_{eq} = 1$ indicates complete equilibration. Gillon & Yakir (2001) report an average leaf disequilibrium in C_4 plants, excluding outliers, of 0.38, while Helliker (2001) estimated Θ_{eq} to range from 0.6 to 0.7 in both leaf-level and whole-plant experiments with the C_4 grass *Andropogon gerardii*. Additionally, large variations in leaf water isotopic composition along the leaf length were reported by Helliker & Ehleringer (2000), further complicating predictions of photosynthetic $C^{18}OO$ exchanges in grasslands.

In this paper, we describe a set of isotopic measurements and simulations in a C_4-dominated tallgrass prairie ecosystem located in north-central Oklahoma, USA. After describing the experimental methods and measurements, we apply a mechanistic land-surface and isotope model (ISOLSM; Riley *et al.*, 2002) to interpret the physiological and biophysical controls on measured $\delta^{18}O$ values of CO_2 and H_2O pools and fluxes. We also demonstrate the importance of incomplete equilibration between leaf water and CO_2 on ecosystem $C^{18}OO$ fluxes.

Materials and methods

Site description

Measurements were made in a tallgrass prairie pasture in Oklahoma, USA ($36°56'N$, $96°41'W$) during three sampling campaigns in 2000: May 6–10, June 4–7, and July 18–21. The site is in a region with various land uses and covers, including crops, sparse trees, and other grasslands; it has not been grazed since 1996, but is burned every spring. The maximum leaf area index

(LAI) is about 3.0 and the maximum net ecosystem exchange during the growing season is about $35\,\mu mol\,m^{-2}\,s^{-1}$. The site and collection of meteorological forcing and flux data are described in detail in Suyker & Verma (2001).

C_4 grasses constituted at least 78% of the species present in a vegetation cover survey conducted in 1997 (Suyker & Verma, 2001). However, this proportion varies seasonally. Still *et al.* (2003a) used night-time ^{13}C measurements to estimate the fraction of ecosystem respiration resulting from C_4-derived carbon. In 2000, these measurements indicated that the C_4 contribution increased from 67% in early spring to 77% in midsummer. Daytime measurements of above-canopy ^{13}C gradients showed a similar seasonal increase in the fraction of net ecosystem exchange attributable to C_4 plants.

CO_2 measurements

Night-time CO_2 Keeling plots

We collected air samples at four heights above the surface (0.5, 1.5, 2.5, and 4.5 m) several times during the night when both plant and heterotrophic respiration were occurring. The 0.5 m sampling level was directly above the grassland canopy. Each air sample was collected over a 2-min interval, so that all four levels were sampled in less than about 10 min. Each set of four samples was used to create a single Keeling plot intercept. Further details of field sampling are described in Still *et al.* (2003a). Air samples were collected and stored in 100 ml glass flasks (Kontes Custom Glass Shop, Hayward, CA, USA) and returned to the Carnegie Institution of Washington for concentration and isotopic analysis. This analysis was conducted using a system that simultaneously measures CO_2 mixing and isotope ratios in small air samples (Ribas-Carbo *et al.*, 2002). The measurement precision for CO_2 concentration with this system is 0.4–0.7 ppm, and for $\delta^{18}O$ values of CO_2 is 0.05‰.

Using the night-time data, we constructed mixing plots (Keeling plots) to estimate the isotopic composition of the net ecosystem CO_2 flux, δ_e (‰). This approach (Keeling, 1958; Keeling, 1961) assumes that the system can be represented as a simple mixture of atmospheric CO_2 and the CO_2 produced by ecosystem respiration. The intercept from a linear regression between the $\delta^{18}O$ value of the CO_2 concentration and the reciprocal of the CO_2 concentration provides an estimate of the isotopic composition of the respiration source. We used a geometric mean regression that incorporates errors in both the concentration and isotopic composition measurements to calculate the intercept (Friedli *et al.*, 1987; Sokal & Rohlf, 1995;

Flanagan *et al.*, 1996; Bowling *et al.*, 1999; Harwood *et al.*, 1999; Bowling *et al.*, 2001), while the standard error of the regression intercept was calculated with a Model I formula (Sokal & Rohlf, 1995; Laws, 1997). We report isotopic values in per mil (‰), with CO_2 isotopic concentration and flux ratios calculated relative to the standard Vienna Pee Dee belemnite (V–PDB-CO_2), and H_2O isotopic concentration and flux ratios calculated relative to Vienna-Standard Mean Ocean Water (V–SMOW).

Daytime discrimination

We sampled daytime CO_2 concentration and $\delta^{18}O$ values at the highest (4.5 m) and lowest (0.5 m) tower levels during the 2000 growing-season. The sample collection was the same as that used for night-time collections, except that only two levels were sampled for each measurement.

The average measured CO_2 concentrations and isotopic ratios sampled at each height during a one to three hour period were used for each discrimination calculation. On a typical day, fewer than 10 gradient pairs with sufficient concentration and isotope gradients could be sampled due to strong winds at the site. The net ecosystem discrimination against $C^{18}OO$, Δ_e^{18} (‰), was calculated as (derived in Still *et al.*, 2003a); see also Evans *et al.* (1986); Lloyd & Farquhar (1996):

$$\Delta_e^{18} = \frac{-1000C_H(\delta_H - \delta_L)}{1000(C_H - C_L) + (\delta_H C_H - \delta_L C_L)}, \qquad (1)$$

where C_H and C_L (μmol m^{-3}) are the CO_2 concentrations at the high and low sampling points, respectively, and δ_H and δ_L (‰) are the $\delta^{18}O$ values of CO_2 at the high and low sampling points, respectively.

Soil-surface CO_2 flux

We measured the $\delta^{18}O$ value of the soil-surface CO_2 flux on two occasions in July 2000. The measurement protocol was designed to minimize pressure artifacts (Lund *et al.*, 1999) and to average over the small-scale variation in C_3 and C_4 abundance. We used a modified Licor 6400 soil respiration system (Still *et al.*, 2003a). A balloon was placed on the inside of the chamber over the pressure equalization port and a septum was attached so that air could be withdrawn from the chamber through a small column of magnesium perchlorate into pre-evacuated 100 mL flasks. When a sample was taken, atmospheric air flowed into the balloon, equalizing the pressure inside and outside the chamber. The chamber was placed on open patches of soil between grass tussocks. Before sampling, respired CO_2 was allowed to accumulate in the chamber for a time (the same for each replication) sufficient to reach a concentration of approximately 700 ppm. Seven flasks

from the chamber were taken, one each from seven separate soil patches. Two flasks were also filled with ambient air (one at the beginning and one at the end of the sampling sequence). The data were combined for Keeling plot analysis (geometric mean regression, nine points per curve) to obtain a flux-weighted average of the isotopic composition of CO_2 respired from the sampled surface area.

Using the method described in Miller *et al.* (1999), we calculated the impact of invasion (excess chamber CO_2 diffusing into the soil, equilibrating with soil water, and diffusing back into the chamber) on the soil-surface isoflux to be small (less than 0.5%), primarily because soil moisture in the top 15 cm was low at the time of this measurement (less than 25% water-filled pore space).

H_2O measurements

Atmospheric water vapor

Atmospheric water vapor samples were collected and analyzed for ^{18}O composition. The water vapor mixing ratio was determined by averaging the micrometeorological measurements at each height over the sampling period. For ^{18}O composition, water vapor was collected from four heights so that each Keeling plot consisted of four samples. The sampling methodology is described in detail in Helliker *et al.* (2002). Briefly, atmospheric air was pulled through a dry-ice-cooled glass condenser for 15 min. The samples were then sealed and shipped to the SIRFER laboratory at the University of Utah (http://ecophys.biology.utah.edu/sirfer.html). Pure CO_2 was injected into condensers (to a final concentration of 10%) and allowed to equilibrate for 48 hours. The $\delta^{18}O$ value was determined by on-column injection through a continuous flow isotope ratio mass spectrometer. Keeling plots for water vapor were calculated analogously to those for CO_2.

Leaf and soil water

Soil water, bulk leaf water, and plant stem water were collected and analyzed for ^{18}O composition. Soil water was sampled with a soil corer to 20 cm depth. We subsampled each core in four intervals: 0–2.5, 2.5–5, 5–10, and 10–20 cm. These soil plugs were placed in glass vials, sealed with parafilm, and stored for isotopic analysis. The leaf water isotopic composition was determined by collecting upper leaves from the dominant plants (C_3: *Solidago missouriensis*; C_4: *Andropogon gerardii*, *Panicum virgatum*, and *Sorghastrum nutens*) at mid-day and storing them in glass vials as with the soil samples.

The leaf and soil samples were analyzed at SIRFER at the University of Utah. Water was extracted from the sample with cryogenic distillation and its

^{18}O composition was determined by the CO_2–H_2O equilibration method of Socki *et al.* (1992) with modifications described in Helliker & Ehleringer (2000).

ISOLSM simulations

ISOLSM couples the land-surface model LSM1.0 (Bonan, 1996) with modules that predict the ^{18}O composition of canopy water vapor, leaf water, and vertically resolved soil water; CO_2 oxygen isotope exchanges with soil and leaf water; leaf photosynthetic $C^{18}OO$ fluxes; soil CO_2 and $C^{18}OO$ diffusive fluxes (including abiotic soil exchange); and ecosystem exchange of $H_2^{18}O$ and $C^{18}OO$ with the atmosphere. A detailed description of the processes simulated in ISOLSM can be found in Riley *et al.* (2002). Briefly, the depth-resolved ^{18}O isotopic ratio of soil water is solved by an explicit numerical solution to the $H_2^{18}O$ mass balance. The model accounts for equilibrium fractionation during evaporation and fractionation through the laminar layer at the soil surface. Rain and irrigation inputs are treated as boundary conditions on the soil water ^{18}O balance. A semi-implicit numerical scheme is used to simulate the soil-gas diffusion and CO_2 interactions with ^{18}O in the soil water. For the simulations shown here, the model calculates the energy balance, photosynthetic CO_2 flux, soil moisture and temperature, and the $\delta^{18}O$ value of soil moisture with a time step of 100 s, while the soil-gas diffusion model uses a time step of 20 s. Predictions of the $\delta^{18}O$ value of leaf water, δ_l (‰), are based on the predicted stem water and canopy water vapor isotopic composition and the Craig–Gordon model (Craig & Gordon, 1965) with modifications for leaves as described by Flanagan *et al.* (1991). The canopy water vapor ^{18}O composition is determined diagnostically based on fluxes from the atmosphere, leaves, and the soil surface. As mentioned earlier, incomplete equilibration between leaf water and CO_2 can occur in C_4 grass leaves as a result of low CA activity. Gillon & Yakir (2000) showed that a reasonable approximation for leaf disequilibrium is $\Theta_{eq} = \Delta_c/\Delta_{eq}$, where $\Delta_c = (R_c/R_a - 1)1000$, $\Delta_{eq} = (R_{eq}/R_a - 1)1000$, and R_a, R_c, and R_{eq} represent the isotopic ratios of the background atmosphere, chloroplast CO_2, and CO_2 in equilibrium with leaf water, respectively. We apply these relationships to calculate an equivalent $\delta^{18}O$ value of leaf internal CO_2 that reflects the reduced leaf discrimination due to disequilibrium.

We used measurements from the site to specify soil characteristics and the vertical root distribution. ISOLSM is forced with measurements of air temperature, wind speed, CO_2 concentration, vapor pressure, downward short-wave and long-wave radiation, precipitation or irrigation amount and its isotopic ratio,

and the $\delta^{18}O$ value of above-canopy vapor and CO_2. We conducted the simulations presented here assuming a 100% C_4 canopy, as C_4 plants dominate the net ecosystem exchange during the growing season. Since we did not have continuous measurements of the isotopic composition of atmospheric vapor, we assumed a value 7‰ less than the predicted stem water isotopic composition. Actual values are impacted by many factors other than evapotranspiration (e.g., horizontal and vertical atmospheric advection), and show diurnal variations of up to 4‰ (Helliker *et al.*, 2002). We also lacked measurements of the isotopic composition of above-canopy CO_2 and assumed a constant value of 0‰ for the results shown here, although diurnal variations of up to 2‰ are common (Helliker *et al.*, 2002). We test the sensitivity of model predictions to variations in the $\delta^{18}O$ values of atmospheric CO_2 and H_2O below.

Results and discussion

In this section, we present experimental results and discuss comparisons between measured and simulated latent heat, sensible heat, and CO_2 fluxes; the ^{18}O composition of water in leaves and stems; vertically resolved soil water ^{18}O composition; and $H_2^{18}O$ and $C^{18}OO$ exchanges with the atmosphere. We also apply ISOLSM to examine biological and physical controls on these exchanges.

Ecosystem CO_2 and latent and sensible heat fluxes

Model predictions of ecosystem CO_2 and latent and sensible heat fluxes impact predictions of ecosystem $H_2^{18}O$ and $C^{18}OO$ stocks and fluxes. For example, sustained inaccuracy in the predicted ecosystem latent heat flux can result in inaccurate predictions of near-surface soil water isotopic composition. Such errors can propagate to impact stem and leaf water isotopic composition predictions and therefore the ecosystem exchanges of $C^{18}OO$. The model accurately simulated the magnitude and dynamics of CO_2 and latent and sensible heat fluxes over the growing season. For example, Fig 1(a) and (b) show comparisons between measured and modeled fluxes over a 10-day period beginning May 1, 2000.

Isotopic composition of ecosystem water pools

Figure 2 shows the predicted and measured depth-resolved soil water isotopic composition over the 3-month period. We initialized the modeled soil water isotopic composition using measurements taken at the beginning of May 2000. The model reasonably predicts
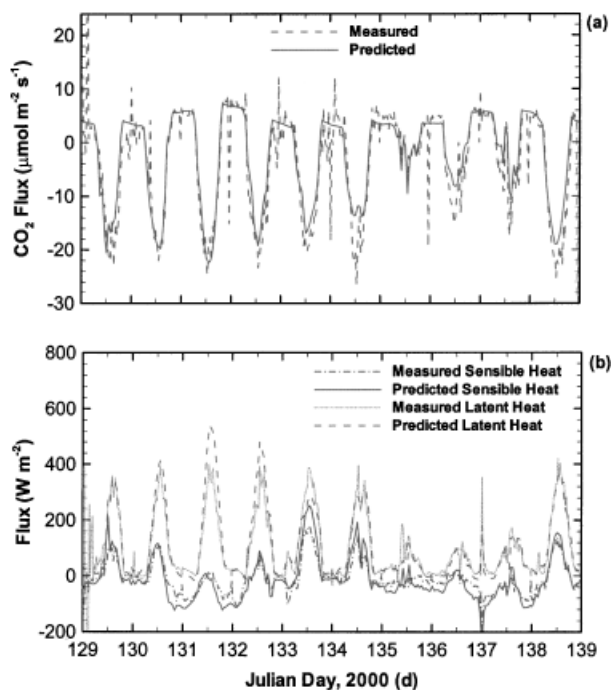
Fig. 1 Measured and predicted ecosystem (a) CO_2 fluxes and (b) latent and sensible heat fluxes for a 10-day period in May 2000. Spikes in the measured night-time CO_2 fluxes are likely due to transient perturbations in the boundary layer.
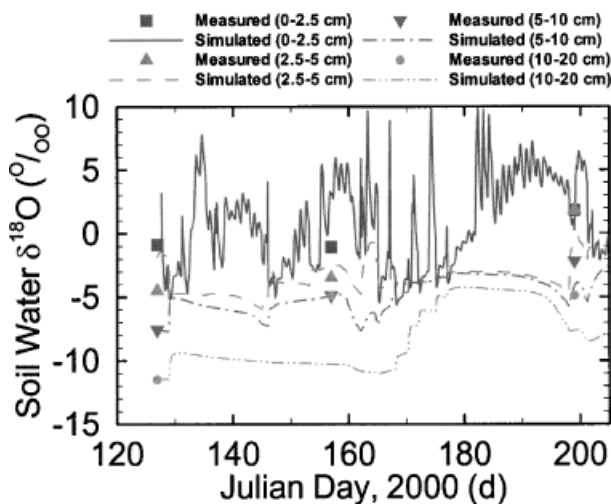

Fig. 2 Measured and predicted soil water ^{18}O isotopic composition over four depth intervals. The top soil layer $\delta^{18}O$ value responds rapidly to surface evaporation and precipitation. $\delta^{18}O$ values are relative to the V-SMOW standard.

the $\delta^{18}O$ value of soil water measured in the subsequent periods. The 10–20 cm soil layer water isotopic composition is predicted to be ~5 and 3‰ too light in the June and July measurement periods, respectively, while the soil water isotopic composition between 2.5 and 5 cm is

predicted to be ~2‰ too light in the July measurement period. The predictions are dependent on the assumed rooting activity depth profile and the $\delta^{18}O$ value of atmospheric water vapor, as described in Riley *et al.* (2002). The impact of errors in the rooting activity is difficult to evaluate since the activity profile at this site is not known. Errors in the imposed atmospheric water vapor $\delta^{18}O$ value could easily result in an error in the predicted near-surface soil water isotopic composition of 2‰ after 3 months of simulation.

The temporal resolution of the measurements shown in Fig. 2 does not allow us to conclude that predicted diurnal variations in soil water isotopic composition between 0 and 2.5 cm, which are as large as 5‰, are accurate. However, we observed comparable diurnal variability in measurements of the $\delta^{18}O$ value of near-surface soil water taken in the summer of 2001 in a sorghum field in Oklahoma (data not shown). These variations are driven by soil evaporation, and are largest when evaporation is large, e.g., following precipitation. Nonetheless, more diurnal measurements of soil water ^{18}O composition are required to test these model predictions adequately. Accurately predicting the near-surface soil water isotopic composition is important since it influences the isotopic composition of the net soil-surface CO_2 and H_2O fluxes.

Predicted and measured leaf and stem water isotopic compositions for the dominant C_4 grasses are shown in Fig. 3 for the 3 days in May, June, and July for which we have measurements. δ_l and the $\delta^{18}O$ value of stem water are accurately predicted in May and July, while δ_l is predicted to be ~3‰ too heavy in the June sampling. The predicted δ_l typically increases from early morning to mid-afternoon by between 10‰ and 20‰, and then relaxes back to a night-time steady value. We have observed similar patterns and magnitudes of diurnal variation in sorghum leaf water ^{18}O composition in this area (data not shown). The leaf water isotopic composition is substantially more variable than that of soil water (particularly deeper than 5 cm; Fig. 2) over the afternoon, resulting in more variable $\delta^{18}O$ values of leaf CO_2 fluxes than of soil CO_2 fluxes.

Ecosystem $H_2^{18}O$ fluxes

The predicted and measured evapotranspiration (ET) flux isotopic composition is shown in Fig. 4 for the 3 days when H_2O Keeling plots were available. The predicted ecosystem water flux isotopic composition shows strong diurnal variation, consistent with the variable soil evaporation isotopic composition and fraction of total ET attributable to soil evaporation. The $\delta^{18}O$ value of the net ecosystem vapor flux will be more variable the larger the contribution of soil
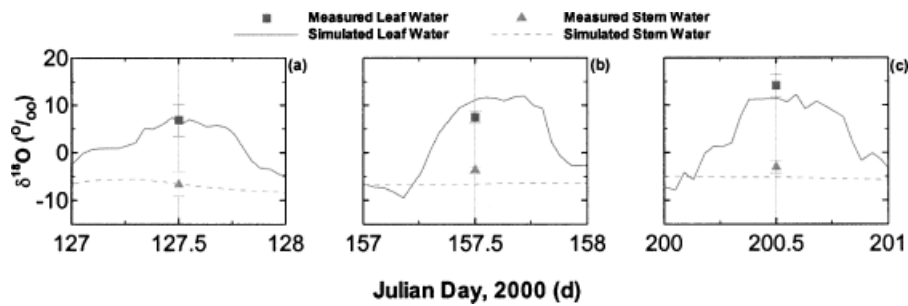
Fig. 3 Measured and predicted leaf and stem water ^{18}O isotopic composition. The predicted stem water ^{18}O composition represents a convolution over depth of rooting activity and soil water ^{18}O composition. Leaf water δ^{18}O values depend on leaf temperature, δ^{18}O value of stem water, and canopy airspace vapor concentration and δ^{18}O value. δ^{18}O values are relative to the V-SMOW standard.
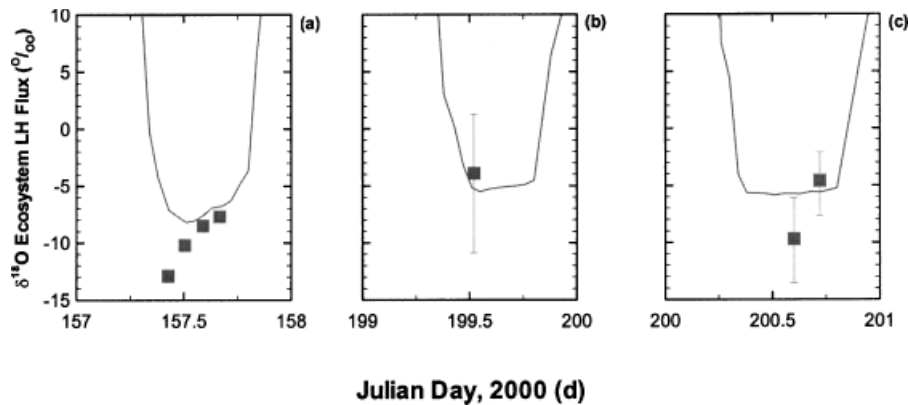

Fig. 4 Measured and predicted ^{18}O isotopic composition of ecosystem latent heat flux (soil evaporation and transpiration). For figure clarity, we omitted the 95% confidence intervals on (a) which, from left to right are: (2.5, − 27.2), (2.6, − 22.7), (3.1, − 19.9), and (0.5, − 15.5). When transpiration dominates the latent heat flux, the ecosystem isotopic composition more closely matches the stem water ^{18}O composition. As the soil evaporative flux becomes a larger fraction of the ecosystem latent heat flux, the ecosystem signal becomes more variable. δ^{18}O values are relative to the V-SMOW standard.

evaporation to the total ET flux. δ^{18}O values of canopy and above-canopy atmospheric vapor and soil-surface evaporation and transpiration are shown for a typical day in Fig. 5. The soil evaporation isotopic composition is typically lightest at about 11 in the morning and increases throughout the day. This increase is caused by the concurrently increasing near-surface soil water isotopic composition and soil-surface equilibrium-partitioning coefficient (due to increased soil temperature). The perturbations in canopy water vapor and soil evaporation δ^{18}O values at about day 180.6 occur because of a rapid change in measured downward short-wave radiation over this period, probably caused by clouds. At any particular time, the canopy water vapor isotopic composition depends on H_2^{18}O and H_2O fluxes between the canopy air and (1) overlying atmosphere, (2) leaves, and (3) soil surface (see Eqn (11) of Riley *et al.* (2002)). Typically, the predicted canopy air space vapor isotopic composition in the morning is

close to that of the background above-canopy vapor, increases until about mid-day as a result of the heavier transpiration flux, and then returns to the background value as the ecosystem latent heat flux diminishes in the late afternoon.

Soil respiration C^{18}OO fluxes

The measured and predicted δ^{18}O values of soil-respired CO_2 are presented in Fig. 6. In these simulations, we imposed soil respiration profiles that decay exponentially with depth. We assume that the root respiration profile follows the root distribution profile with an *e*-folding depth, z_0 (m), of 0.2 m, and that the microbial respiration has a profile defined by $z_0 = 0.05$ m. Thus, about 75% of the predicted soil respiration occurs in the top 15 cm of soil. In reality, the depth distribution of respiration will depend on the distribution of root activity, soil moisture and
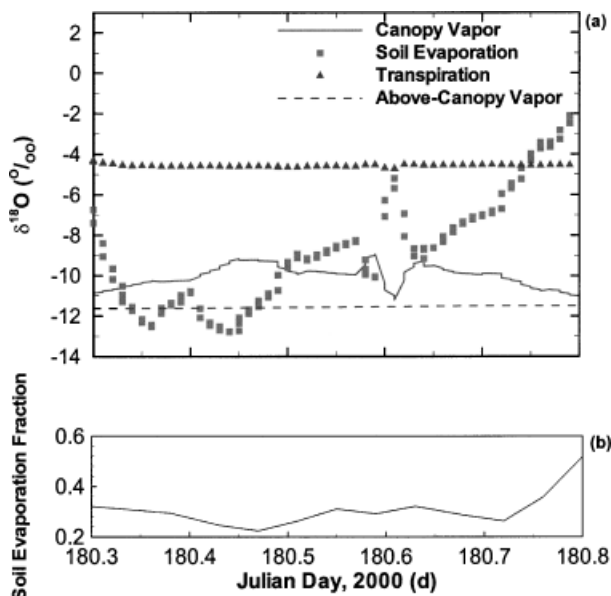
Fig. 5 (a) Predicted ^{18}O isotopic composition of canopy vapor, soil evaporation, transpiration, and above-canopy vapor for a single daytime period. The canopy vapor isotopic composition increases during the day due to the heavier transpiration flux, and then returns to the above-canopy composition as the ecosystem latent heat flux diminishes. (b) Fraction of evapo-transpiration due to soil evaporation. δ^{18}O values are relative to the V-SMOW standard.
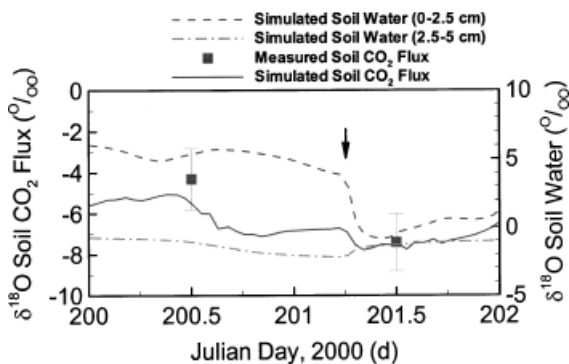

Fig. 6 Measured and predicted ^{18}O isotopic composition of the net soil-surface CO_2 flux (left ordinate) and predicted δ^{18}O value of soil water between 0–2.5 cm and 2.5–5 cm (right ordinate). The arrow indicates a small precipitation event with a δ^{18}O value of − 2.6‰. Predicted and measured δ^{18}O values of the net soil-surface CO_2 flux reflect the relatively lighter soil water in the 0–2.5 cm layer after the precipitation event. Soil water δ^{18}O values are relative to the V-SMOW standard; CO_2 flux δ^{18}O values are relative to the V-PDB-CO_2 standard.

temperature, and microbial substrate availability, among others. The δ^{18}O value of the net soil-surface CO_2 flux is sensitive to the depth distribution of CO_2 production. For example, if a larger fraction of respiration occurs near the surface, the δ^{18}O value of the net soil-surface

CO_2 flux will become more enriched as a result of equilibration with more enriched near-surface soil water.

The decrease in the measured δ^{18}O value of soil-respired CO_2 between days 200 and 201 is caused by a small precipitation event with a δ^{18}O value of − 2.6‰ (indicated by the arrow in Fig. 6). This precipitation input is reflected in the simulated δ^{18}O value of soil water as a decline in the top soil layer and as a small increase in the second soil layer. The small increase in the δ^{18}O value of soil water in the 2.5–5 cm layer results from advection of the heavier soil water (before the precipitation event) from 0–2.5 cm. As the CO_2 diffuses through the top soil layer, it interacts with this lighter soil water and thereby acquires a lighter isotopic composition. Note that this result contradicts the observation of Miller *et al.* (1999) that the δ^{18}O value of water in the top 5 cm of soil does not substantially impact the δ^{18}O value of the soil-surface CO_2 flux. The decrease in the δ^{18}O value of soil-respired CO_2 resulting from the precipitation event is accurately captured by ISOLSM. In general, the impact of a precipitation event on the δ^{18}O value of soil-respired CO_2 depends on the precipitation flux, δ^{18}O value of precipitation and antecedent soil moisture, and the fraction of soil respiration occurring in the near-surface soil.

Ecosystem $C^{18}OO$ fluxes

Figures 7(a)–(c) show predicted and measured δ^{18}O values of the net ecosystem CO_2 flux (Keeling plot intercepts) for the three periods where measurements were made (predicted values are shown when the magnitude of the ecosystem CO_2 flux is greater than 2 μmol m^{-2} s^{-1}). Three simulation scenarios are shown: the first assumes complete equilibration within the leaf ($\Theta_{eq} = 1.0$) and the second and third assume $\Theta_{eq} = 0.5$ and 0.35, respectively. In Fig. 7, only measurements with R^2 values greater than 0.6 and CO_2 gradients (between 0.5 and 4.5 m height) greater than 15 ppm are included (Table 1).

The δ^{18}O value of the predicted ecosystem CO_2 flux varied substantially during the day and between days due primarily to variations in δ_l (also shown in Fig. 7) and leaf internal CO_2 concentration, C_i (μmol m^{-3}). At night the predicted CO_2 flux isotopic composition remained relatively constant since the soil water isotopic composition and soil temperature are relatively constant. The sharp transitions in the δ^{18}O values of the net ecosystem CO_2 flux during the morning and evening occur when the system switches between being dominated by respiration and photosynthesis. During the day, photosynthetic uptake and retrodiffusion dominate ecosystem CO_2 and $C^{18}OO$ exchange. Lower
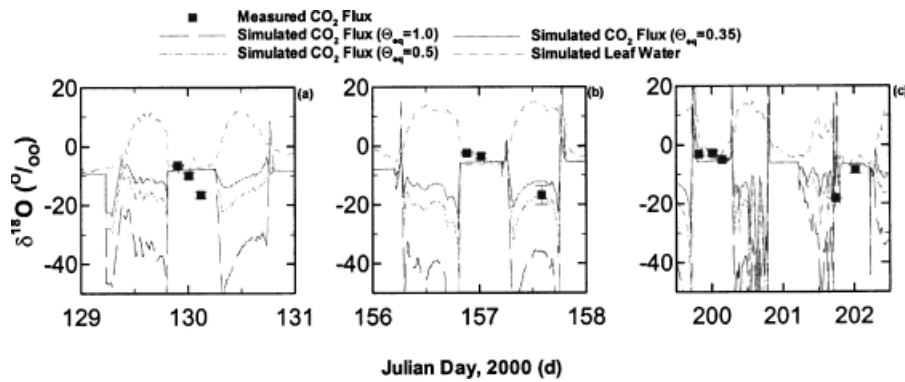
Fig. 7 Measured Keeling plot intercepts, predicted δ^{18}O value of the ecosystem CO_2 flux, and predicted δ_l for five measurement periods. Simulated results are shown for three levels of leaf disequilibrium (Θ_{eq} = 1.0, 0.5, and 0.35). Note that a negative δ^{18}O value of the daytime ecosystem flux enriches the atmosphere. Leaf water δ^{18}O values are relative to the V-SMOW standard; CO_2 flux δ^{18}O values are relative to the V-PDB-CO_2 standard.

Table 1 R^2 values and differences in CO_2 concentrations between 0.5 and 4.5 m for the night-time CO_2 Keeling plot intercepts shown in Fig. 7

Date	Time (hours)	ΔCO_2 (ppm)	R^2
5/9/2000	21:37	65	0.99
5/10/2000	12:10	25	0.97
5/10/2000	2:50	22	0.99
6/5/2000	21:11	128	0.83
6/6/2000	12:23	118	0.62
7/18/2000	21:37	47	0.90
7/19/2000	12:20	118	0.98
7/19/2000	3:32	31	0.85
7/20/2000	21:47	16	0.72
7/21/2000	12:27	9	0.97

values of Θ_{eq} resulted in significantly more positive δ^{18}O values of daytime ecosystem CO_2 fluxes. Note that a negative δ^{18}O value of the daytime ecosystem CO_2 flux enriches the atmosphere.

Using a two-component mixing model (Keeling plot) to estimate the δ^{18}O value of respired CO_2 from measurements can be misleading, since (1) changes in the δ^{18}O value of ecosystem respiration can occur independently of changes in CO_2 concentration and (2) the water pools driving these isotopic changes can be spatially and temporally heterogeneous (Amundson *et al.*, 1998; Tans, 1998). As a result, extrapolation of the linear regression to infinite CO_2 concentration may not give an accurate estimate of the isotopic composition of respired CO_2. This decoupling of atmospheric CO_2 mole fraction and the isotopic composition of respired CO_2 can be caused by temporal changes in the leaf or soil water isotopic compositions over the measurement period. δ_l is more likely to change over the night than

the δ^{18}O value of soil water (particularly below $\sim$5 cm depth). It is unlikely that changes in leaf and soil water isotopic compositions affected our measurements at a particular time because each of our night-time estimates was based on measurements collected along a vertical spatial gradient over a short time interval. However, this effect can impact our interpretation of measurements throughout the night, as discussed below. The abiotic invasion of $C^{18}OO$ into soils and horizontal atmospheric advection can also impact the expected linear Keeling plot relationship. These potential confounders indicate that care must be taken when testing the accuracy of model predictions against δ^{18}O Keeling plot intercepts. Despite these concerns, the majority of our Keeling plots seem to follow the two-component model assumption, as demonstrated by the high R^2 values shown in Table 1.

The May 2000 ecosystem CO_2 flux isotopic compositions are notable since the Keeling plot intercepts tend toward more negative values throughout the night, contrary to model predictions. We believe that this measured trend is real. The CO_2 gradients in these Keeling plots (Table 1) are less than the threshold recommended by Pataki *et al.* (2003). However, that recommendation was based on the decrease in standard error of Keeling plot intercepts with increasing CO_2 gradients. The threshold they recommend (75 ppm) corresponds to a standard error of the intercept of 1‰; the standard errors of our three night-time intercepts are 0.2‰, 0.9‰, and 1.0‰, despite the relatively small CO_2 gradients. The inability of the model to capture this night-time trend may reflect (a) more rapid relaxation than is predicted by the model of leaf water isotopic composition back to the relatively depleted source water, thereby impacting leaf dark respiration; (b) an inaccurate prediction of night-time leaf stomatal
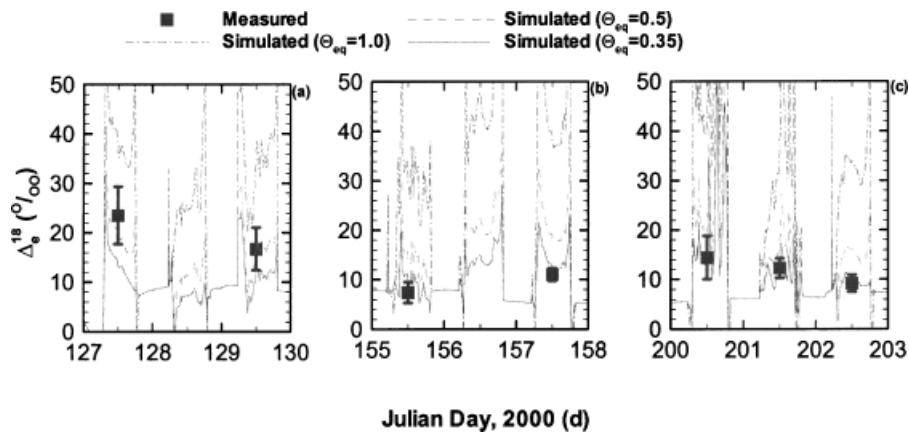
Fig. 8 Measured and predicted ecosystem discrimination for seven daytime periods. Predictions are shown for three levels of leaf disequilibrium (Θ_{eq} = 1.0, 0.5, and 0.35). Θ_{eq} values of 0.5 or 0.35 force model predictions closer to measured values (see text for caveats). From left to right, the number of flask pairs for each calculation is 5, 5, 5, 9, 3, 5, and 6. Discrimination values are relative to the V-PDB-CO_2 standard.

conductance; (c) changes in the isotopic composition of soil respiration not accurately predicted by the model; (d) incorrect prediction of invasion due to inaccurate estimates of the $\delta^{18}O$ value of net soil-surface CO_2 fluxes; or (e) advection (i.e., temporal heterogeneity in background atmospheric $\delta^{18}O$ values resulting from advection of air from adjacent areas). We do not have sufficient information to evaluate the relative impact of these mechanisms on the trend in these measurements.

Daytime discrimination
The measured (Eqn (1)) and predicted daytime ecosystem discrimination values (Δ_e^{18}) are shown in Figs 8(a)–(c). The predicted Δ_e^{18} is calculated as

$$\Delta_e^{18} = \left(\frac{R_a}{R_e} - 1\right)1000 = \frac{\delta_a - \delta_e}{1 + \delta_e/1000}, \quad (2)$$

where R_e (–) is the isotopic ratio of the net ecosystem CO_2 flux. Comparing predicted and measured ecosystem discrimination indicates that leaf disequilibrium may be substantial. In May, June, and July, Θ_{eq} values of 0.5, 0.35, and 0.35, respectively, force model predictions closer to measured values. Care must be taken in interpreting this observation since other modeled state variables (e.g., δ_l and C_i) also have substantial impacts on Δ_e^{18} and may be inaccurately represented in the model. For example, our modeled δ_l is higher than that observed in June, which will result in an overestimate of leaf discrimination. Further, our assumption of isotopic steady state in the leaf may result in an overestimate of δ_l during transient environmental conditions. Errors in simulating C_i are potentially more troublesome due to the non-linear relationship between C_i and leaf discrimination against $C^{18}OO$ (Farquhar &
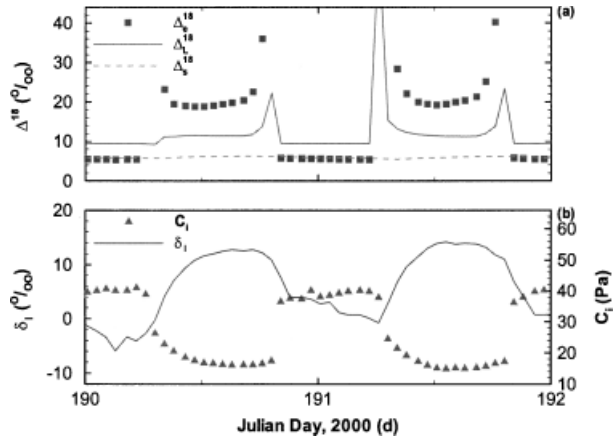

Fig. 9 Characteristic diurnal patterns of Δ_e^{18}. (a) Predicted ecosystem, soil, and leaf discrimination for $\Theta_{eq} = 0.5$. (b) Predicted δ_l and C_i. Daytime ecosystem discrimination follows the pattern of leaf discrimination with a relatively constant offset due to soil discrimination. Discrimination values are relative to the V-PDB-CO_2 standard.

Lloyd, 1993). C_3 plants have higher C_i than C_4 plants and, as a result, larger leaf discrimination values. Therefore, the diminishing proportion of C_3 plants over the season may also cause the progression toward lower measured Δ_e^{18}; this effect is not included in the modeling predictions shown here.

We examine more closely the factors contributing to the predicted Δ_e^{18} over the course of a single day in Figs 9(a) and (b). In Fig. 9(a), $\Theta_{eq} = 0.5$ and Δ_s^{18} and Δ_L^{18} (‰) represent the net discrimination of $C^{18}OO$ from soil and leaves, respectively, and are calculated analogously to Δ_e^{18}. The predicted δ_l and C_i are shown in Fig. 9(b). The

net ecosystem discrimination increases from $\sim 5‰$ before sunrise to about 20‰, and remains relatively constant until late in the afternoon. The abrupt shifts in the early morning and later afternoon occur as the system transitions between being dominated by photosynthesis and respiration; the net ecosystem isoflux is relatively small during these periods. Note that, although soil 'discrimination' is calculated to be positive, soil respiration typically makes the atmosphere lighter, in contrast to photosynthesis. Diurnal variations in Δ_s^{18} are small. With respect to impacts on Δ_L^{18}, the increase (decrease) in δ_l is opposed by the decrease (increase) in C_i during the morning (afternoon).

Ecosystem isoflux

The ecosystem ^{18}O-isoflux, I (μmol m^{-2} s^{-1}‰), quantifies the net impact of ecosystem fluxes on the atmospheric C^{18}OO content:

$$I = -(F_{al} - F_{la})\delta_{nl} + (F_g + F_{sm})\delta_{sw} + F_s\delta_s, \quad (3)$$

where δ_{nl}, δ_{sw}, and δ_s (‰) are the predicted δ^{18}O values of the net leaf, stem respiration, and net soil-surface CO$_2$ fluxes, respectively; F_{al} and F_{la} (μmol m^{-2} s^{-1}) are the predicted CO$_2$ fluxes into and out of the leaf, respectively; and F_g, F_{sm}, and F_s (μmol m^{-2} s^{-1}) are the predicted growth respiration, stem respiration, and net soil-surface CO$_2$ fluxes, respectively. The three groups of terms on the right-hand side of Eqn (3) describe the net leaf isoflux, above-ground respiratory isoflux, and net soil-surface respiratory isoflux, respectively.

The net leaf isoflux dominates the ecosystem isoflux (Fig. 10), which varies substantially over the course of the day. The predicted photosynthetic CO$_2$ exchange and δ_l each reach their maximum in the middle of the day, thereby reinforcing the net leaf isoflux magnitude. The net soil-surface isoflux is a small fraction of the

ecosystem isoflux for several reasons. First, the net soil-surface CO$_2$ flux is a small fraction of the ecosystem CO$_2$ flux during this period. This tallgrass system maintains an approximately even carbon balance over the season through losses from soil microbial respiration and fire at other times of the year. In systems where diurnal respiratory and photosynthetic carbon fluxes are more balanced, the soil-surface isoflux will be a more significant contributor to the ecosystem isoflux. Second, the soil water isotopic composition at this site is not strongly depleted relative to the atmosphere (compared with, for example, boreal regions; Flanagan et al., 1997). Third, the mid-day leaf water is strongly enriched due to the low relative humidity and high δ^{18}O value of soil water, thus ensuring a large net leaf isoflux during the day. Finally, photosynthetic fluxes are much higher in productive grasslands than in many other ecosystems.

The relatively low soil moisture in this system leads to a lower effective diffusive fractionation and therefore a relatively enriched net soil-surface CO$_2$ flux. Concurrently, the lower soil moisture may cause a decrease in heterotrophic respiration, thereby reducing the soil isoflux. The net impact of these effects is difficult to discern without a model like ISOLSM that can explicitly simulate the impact of soil moisture and temperature on the CO$_2$ source strength and diffusivity as a function of depth. We will address these interactions and their impact on the δ^{18}O value of the soil-surface CO$_2$ flux in future work.

As mentioned earlier, C$_4$ plants have lower discrimination against C^{18}OO than C$_3$ plants. Thus, all else being equal, soil respiration has a relatively larger impact on the ecosystem isoflux in a C$_4$-dominated system. In a related analysis, we applied ISOLSM to investigate the impact of C$_3$ vs. C$_4$ plant physiology in this tallgrass system (Still et al., 2003b). In addition to the impact on leaf discrimination due to different CO$_2$ concentrations in the leaf stomatal pore, the C$_3$ and C$_4$ systems also have slightly different predicted soil moistures and leaf temperatures for the same meteorological forcing. Soil moisture and leaf temperature impact the soil-surface and leaf isofluxes. In these simulations, the soil isoflux was a larger proportion of the ecosystem isoflux in the C$_4$ system, due primarily to the reduced daytime leaf discrimination.
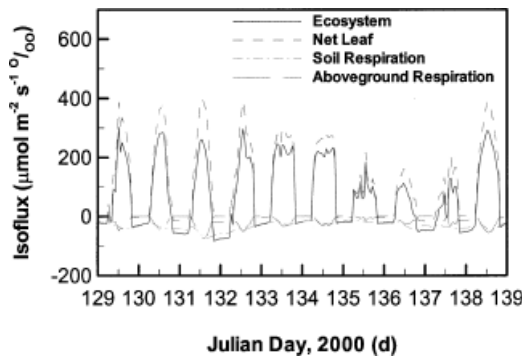
Diurnal variations in the δ^{18}O value of above-canopy CO$_2$

As part of our measurement campaigns in June and July, air samples from the 4.5 m high sampling port were collected in pre-dried and evacuated 100-mL glass flasks every 1.5–3 h and analyzed for their CO$_2$

Fig. 10 Simulated net isotopic forcing (^{18}O-isoflux) for $\Theta_{eq} = 0.5$. The daytime isoflux is dominated by the net leaf isoflux. δ^{18}O values are relative to the V-PDB-CO$_2$ standard.

concentration and oxygen isotope composition (δ_H). Several features are immediately apparent in the isotopic composition data (Figs 11(a) and (c)): an average diurnal cycle with an amplitude of $\sim 1.5‰$, an upward trend in the June period, and a downward trend in the July period. The diurnal cycle amplitude is large and roughly the same size as the interhemispheric δ_a gradient observed by the NOAA-CMDL network (Farquhar *et al.*, 1993; Ciais *et al.*, 1997a, b). During both periods, diurnal variations in δ_H are closely coupled to variations in CO_2 concentration. This tight coupling implies that changes in δ_H are dominated by leaf and soil fluxes and not by changes in the $\delta^{18}O$ value of water pools independently of flux variations. There was no precipitation during these two periods.

An examination of modeled ecosystem ^{18}O-isofluxes (Figs 11(b) and (d)) over these periods shows that the observed $\delta^{18}O$ diurnal cycle in both periods is strongly modulated by leaf photosynthetic ^{18}O-isofluxes, with a small and relatively invariant contribution from soil ^{18}O-isofluxes. The weak trends in observed δ_H in June and July follow trends in the modeled net leaf ^{18}O-isoflux. Unfortunately, a full comparison between modeled ^{18}O-isofluxes and observed δ_H variations is not possible, since δ_H is also influenced by (1) advection of air parcels from adjacent regions, which may have different vegetation cover and soil water ^{18}O composition, and (2) the atmospheric boundary layer height and turbulence conditions, which vary with surface heating and cooling. Coupling ISOLSM to a regional-scale meteorological model that simulates ^{18}O exchanges with CO_2 and H_2O is in progress and will facilitate analyses that include these proceses.

Sensitivity to the $\delta^{18}O$ value of atmospheric CO_2 and H_2O

The simulations described above assume that the $\delta^{18}O$ value of atmospheric water vapor was 7‰ less than the predicted stem water isotopic composition, while the $\delta^{18}O$ value of atmospheric CO_2 was assumed to be constant at 0‰. Measurements at this site indicate that the $\delta^{18}O$ value of above-canopy H_2O and CO_2 can vary by 4‰ and 2‰, respectively, over the day (Helliker
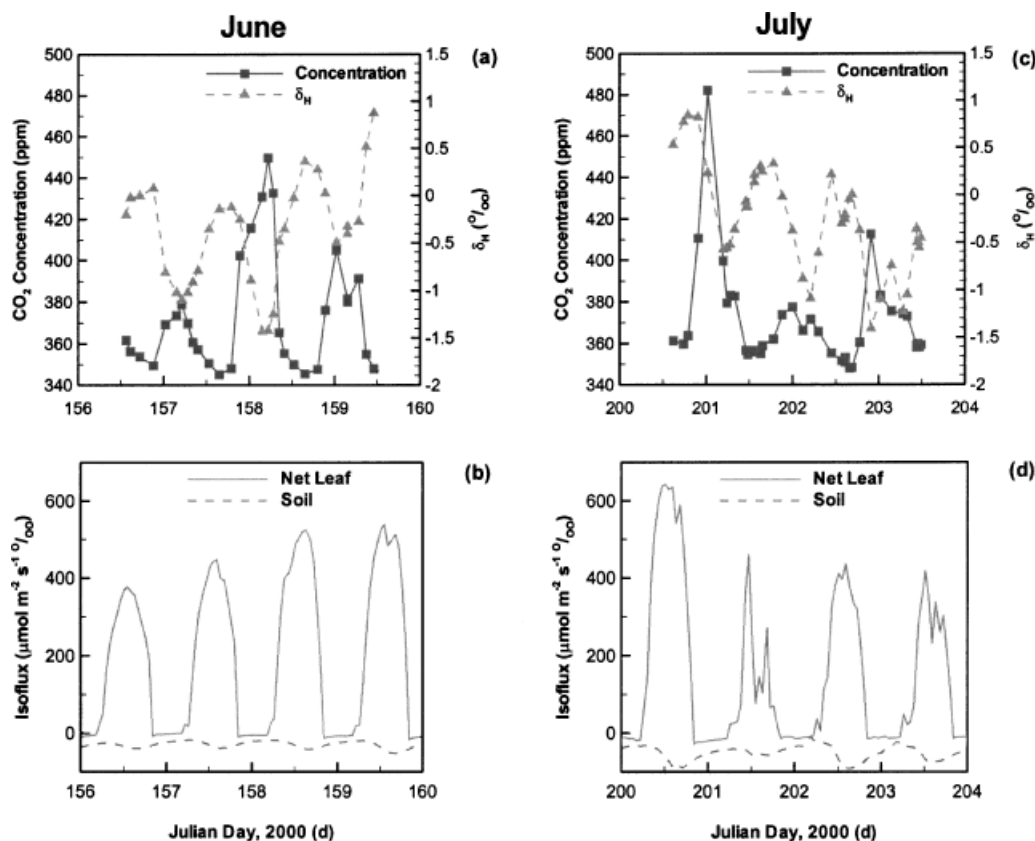

Fig. 11 Measured CO_2 concentration and $\delta^{18}O$ value of CO_2 sampled at 4.5 m (δ_H) during the (a) June 4–7 and (c) July 18–21 measurement campaigns. Simulated net leaf and soil ^{18}O-isofluxes ($\mu mol\,m^{-2}\,s^{-1}\,‰$) are also shown for these two periods (b, d). $\delta^{18}O$ values are relative to the V-PDB-CO_2 standard.

_et al._, 2002). To test the impact of this variation, we imposed changes of these magnitudes while maintaining the average isotopic composition over the day unchanged. The ^{18}O composition of atmospheric H_2O was forced to increase linearly with time between 8:00 and 18:00 hours, with a daily average 7‰ lighter than stem water at 8:00 hours. For the atmospheric isotopic composition of CO_2, we imposed a time-dependent sinusoidal profile with a maximum at 14:00 hours and a daily average of 0‰.

Imposing diurnal variation in the $\delta^{18}O$ value of atmospheric H_2O resulted in effectively no change in the soil water, stem water, and leaf water isotopic compositions, and therefore no change in the $\delta^{18}O$ value of the ecosystem CO_2 flux. Note that changes in the _mean_ $\delta^{18}O$ value of atmospheric H_2O significantly impact the isotopic composition of ecosystem water pools. In contrast, imposing a varying $\delta^{18}O$ value of atmospheric CO_2 resulted in increases of about 2‰ in the $\delta^{18}O$ value of the mid-day ecosystem CO_2 flux, consistent with the increase in the atmosphere-to-leaf $C^{18}OO$ fluxes. Note that an increase in the $\delta^{18}O$ value of the mid-day CO_2 flux will result in a lighter atmosphere. Night-time $\delta^{18}O$ values of the ecosystem CO_2 flux were relatively unaffected by the imposed variability in the $\delta^{18}O$ value of atmospheric CO_2.

Conclusions

In this paper, we present measurements and model predictions of CO_2 fluxes, latent and sensible heat fluxes, leaf and stem $H_2^{18}O$ composition, vertically resolved soil water $H_2^{18}O$ composition, and $H_2^{18}O$ and $C^{18}OO$ ecosystem fluxes in a tallgrass prairie in Oklahoma, USA. Generally, ISOLSM accurately predicted the dynamics and magnitude of these quantities over the 3-month simulation period. The paucity of measurements spanning the diurnal cycle makes it difficult to evaluate the short-term predictions of the model. However, the large predicted diurnal variations in the $\delta^{18}O$ values of ecosystem water pools and resultant $C^{18}OO$ fluxes argue that care must be taken when applying discrete measurements of these quantities to partition net ecosystem fluxes into component gross fluxes.

Continuous $\delta^{18}O$ values of atmospheric CO_2 and H_2O are required inputs to the model, and this information was unavailable for this site. Previous measurements in this system have shown that these quantities can vary substantially over the course of the day. Our simple sensitivity analysis indicated that diurnal variability in the $\delta^{18}O$ value of atmospheric H_2O had a small impact on the isotopic composition of ecosystem water pools, although sustained changes can have significant im-

pacts. Typical variations in the $\delta^{18}O$ value of atmospheric CO_2 increased the mid-day $\delta^{18}O$ value of the ecosystem CO_2 flux by up to 2‰; night-time values were relatively unaffected by the change.

Our simulation results indicate that incomplete equilibration between CO_2 and leaf water is common in this system. Further work is required to quantify accurately the extent of disequilibrium and its impact on net ecosystem $C^{18}OO$ fluxes. The ISOLSM simulations demonstrated that the ecosystem isoflux was dominated by leaf fluxes during the simulation period.

The development of ecosystem isotope models would benefit from further research on the biophysical and physiological controls on plant retro-diffused and soil-respired fluxes, as these fluxes account for the largest uncertainties in the atmospheric $C^{18}OO$ budget. Although leaf retro-diffused fluxes are theoretically well understood for C_3 plants (Farquhar & Lloyd, 1993; Farquhar _et al._, 1993; Ciais _et al._, 1997b), recent experimental evidence suggests a more complicated picture for C_4 plants (Gillon & Yakir, 2000; Helliker & Ehleringer, 2000; Gillon & Yakir, 2001). In particular, the impact of partial equilibration of CO_2 with leaf water and variations in the $\delta^{18}O$ value of water along the leaf need to be addressed. Recent experimental (Miller _et al._, 1999) and theoretical (Tans, 1998; Stern _et al._, 1999; Stern _et al._, 2001; Riley _et al._, 2002) work has advanced our understanding of soil-respired $C^{18}OO$ fluxes; further work is necessary to predict these fluxes across the range of soil types and environmental conditions found in real systems. These types of investigations will enhance our ability to use the $\delta^{18}O$ value of atmospheric CO_2 as a tracer of gross carbon exchanges and a constraint on land-surface biophysical processes.

References

Amundson R, Stern L, Baisden T _et al._ (1998) The isotopic composition of soil and soil-respired CO_2. _Geoderma_, **82**, 83–114.

Bonan GB (1996) A land surface model (LSM version 1.0) for ecological, hydrological, and atmospheric studies: Technical

Description and User's Guide. TN-417 + STR, NCAR, Boulder, CO.

Bowling DR, Baldocchi DD, Monson RK (1999) Dynamics of isotopic exchange of carbon dioxide in a Tennessee deciduous forest. *Global Biogeochemical Cycles*, **13**, 903–922.

Bowling DR, Tans PP, Monson RK (2001) Partitioning net ecosystem carbon exchange with isotopic fluxes of CO_2. *Global Change Biology*, **7**, 127–145.

Ciais P, Denning AS, Tans PP *et al.* (1997a) A three-dimensional synthesis study of delta O-18 in atmospheric CO_2. 1. Surface fluxes. *Journal of Geophysical Research-Atmospheres*, **102**, 5857–5872.

Ciais P, Tans PP, Denning AS *et al.* (1997b) A three-dimensional synthesis study of delta O-18 in atmospheric CO_2. 2. Simulations with the TM2 transport model. *Journal of Geophysical Research Atmospheres*, **102**, 5873–5883.

Craig H, Gordon L (1965) Deuterium and oxygen-18 variations in the ocean and the marine atmosphere. In: *Stable Isotopes in Oceanographic Studies and Paleotemperatures* (ed. Tongiorgi E), pp. 9–130. Spoleto, Italy.

Dawson TE, Mambelli S, Plamboeck AH *et al.* (2002) Stable isotopes in plant ecology [Review]. *Annual Review of Ecology and Systematics*, **33**, 507–559.

Evans JR, Sharkey TD, Berry JA *et al.* (1986) Carbon isotope discrimination measured concurrently with gas exchange to investigate CO_2 diffusion in leaves of higher plants. *Australian Journal of Plant Physiology*, **13**, 281–292.

Farquhar GD, Lloyd J (1993) *Chris's refs*, Carbon and oxygen isotope effects in the exchange of carbon dioxide between terrestrial plants and the atmosphere. In: *Stable Isotopes and Plant Carbon-Water Relations* (ed. Ehleringer JR, Hall AE, Farquhar GD), pp. 47–70. Academic Press, San Diego.

Farquhar GD, Lloyd J, Taylor JA *et al.* (1993) Vegetation effects on the isotope composition of oxygen in atmospheric CO_2. *Nature*, **363**, 439–443.

Flanagan LB, Brooks JR, Varney GT *et al.* (1996) Carbon isotope discrimination during photosynthesis and the isotope ratio of respired CO_2 in boreal forest ecosystems. *Global Biogeochemical Cycles*, **10**, 629–640.

Flanagan LB, Brooks JR, Varney GT *et al.* (1997) Discrimination against (COO)-O-18-O-16 during photosynthesis and the oxygen isotope ratio of respired CO_2 in boreal forest ecosystems. *Global Biogeochemical Cycles*, **11**, 83–98.

Flanagan LB, Comstock JP, Ehleringer JR (1991) Comparison of modeled and observed environmental influences on the Stable oxygen and hydrogen isotope composition of leaf water in *phaseolus-Vulgaris L. Plant Physiology*, **96**, 588–596.

Flanagan LB, Varney GT (1995) Influence of vegetation and Soil CO_2 exchange on the concentration and stable oxygen isotope ratio of atmospheric CO_2 within a Pinus Resinosa Canopy. *Oecologia*, **101**, 37–44.

Francey RJ, Tans PP (1987) Latitudinal variation in oxygen-18 of atmospheric CO_2. *Nature*, **327**, 495–497.

Friedli H, Siegenthaler U, Rauber D *et al.* (1987) Measurements of concentration, $^{13}C/^{12}C$ and $^{18}O/^{16}O$ ratios of tropospheric carbon dioxide over Switzerland. *Tellus Series B-Chemical and Physical Meteorology*, **39**, 80–88.

Gillon JS, Yakir D (2000) Naturally low carbonic anhydrase activity in C-4 and C-3 plants limits discrimination against (COO)-O-18 during photosynthesis. *Plant Cell and Environment*, **23**, 903–915.

Gillon JS, Yakir D (2001) Influence of carbonic anhydrase activity in terrestrial vegetation on the O-18 content of atmospheric CO_2. *Science*, **291**, 2584–2587.

Harwood KG, Gillon JS, Griffiths H *et al.* (1998) Diurnal variation of Delta(CO_2)-C-13, Delta(COO)-O-18-O-16 and evaporative site enrichment of delta(H_2O)-O-18 in Piper aduncum under field conditions in Trinidad. *Plant Cell and Environment*, **21**, 269–283.

Harwood KG, Gillon JS, Roberts A *et al.* (1999) Determinants of isotopic coupling of CO_2 and water vapour within a *Quercus petraea* forest canopy. *Oecologia*, **119**, 109–119.

Helliker BR (2001) *Oxygen Isotopes in C3 and C4 grasses.* Ph.D. Dissertation. University of Utah, Salt Lake City, UT.

Helliker BR, Ehleringer JR (2000) Establishing a grassland signature in veins: O-18 in the leaf water of C-3 and C-4 grasses. *Proceedings of the National Academy of Sciences of the United States of America*, **97**, 7894–7898.

Helliker BR, Roden JS, Cook C *et al.* (2002) A rapid and precise method for sampling and determining the oxygen isotope ratio of atmospheric water vapor. *Rapid Communications in Mass Spectrometry*, **16**, 929–932.

Hesterburg R, Siegenthaler U (1991) Production and stable isotopic composition of CO_2 in soil near Bern, Switzerland. *Tellus Series B-Chemical and Physical Meteorology*, **43**, 197–205.

Keeling CD (1958) The concentration and isotopic abundances of atmospheric carbon dioxide in rural areas. *Geochimica Et Cosmochimica Acta*, **13**, 322–334.

Keeling CD (1961) The concentrations and isotopic abundances of atmospheric carbon dioxide in rural and marine air. *Geochemica et Cosmochimica Acta*, **24**, 277–298.

Laws E (1997) *Mathematical Methods for Oceanographers*. John Wiley and Sons, Inc., New York.

Lloyd J, Farquhar GD (1996) The CO_2 dependence of photosynthesis, plant growth responses to elevated atmospheric CO_2 concentrations and their interaction with soil nutrient status. I. General principals and forest ecosystems. *Functional Ecology*, **10**, 4–33.

Lund CP, Riley WJ, Pierce LL *et al.* (1999) The effects of chamber pressurization on soil-surface CO_2 flux and implications for NEE measurements under elevated CO_2. *Global Change Biology*, **5**, 269–282.

Miller JB, Yakir D, White JWC *et al.* (1999) Measurement of O-18/O-16 in the soil-atmosphere CO_2 flux. *Global Biogeochemical Cycles*, **13**, 761–774.

Pataki DE, Ehleringer JR, Flanagan LB *et al.* (2003) The application and interpretation of Keeling plots in terrestrial carbon cycle research – art. no. 1022. *Global Biogeochemical Cycles*, **17**, 1022.

Peylin P, Ciais P, Denning AS *et al.* (1999) A 3-dimensional study of delta O-18 in atmospheric CO_2: contribution of different land ecosystems. *Tellus Series B-Chemical and Physical Meteorology*, **51**, 642–667.

Ribas-Carbo M, Still C, Berry J (2002) Automated system for simultaneous analysis of delta C-13, delta O-18 and CO_2 concentrations in small air samples. *Rapid Communications in Mass Spectrometry*, **16**, 339–345.

Riley WJ, Still CJ, Torn MS *et al*. (2002) A mechanistic model of H$_2^{18}$O and C^{18}OO fluxes between ecosystems and the atmosphere: model description and sensitivity analyses. *Global Biogeochemical Cycles*, **16**, 1095–1109.

Socki RA, Karlsson HR, Gibson EK (1992) Extraction technique for the determination of oxygen-18 in water using preevacuated glass vials. *Analytical Chemistry*, **64**, 829–831.

Sokal RR, Rohlf FJ (1995) Biometry: The Principles and Practice of Statistics in Biological Research. W.H. Freeman and Company, New York.

Stern LA, Amundson R, Baisden WT (2001) Influence of soils on oxygen isotope ratio of atmospheric CO$_2$. *Global Biogeochemical Cycles*, **15**, 753–759.

Stern LA, Baisden WT, Amundson R (1999) Processes controlling the oxygen isotope ratio of soil CO$_2$: Analytic and numerical modeling. *Geochimica Et Cosmochimica Acta*, **63**, 799–814.

Still CJ, Berry JA, Ribas-Carbo M, *et al*. (2003a) The contribution of C$_3$ and C$_4$ plants to the carbon cycle of a tallgrass prairie: an isotopic approach. *Oecologia*, **136**, 347–359.

Still CJ, Riley WJ, Helliker BR, *et al* (2003b) Simulation of ecosystem oxygen-18 CO$_2$ isotope fluxes in a tallgrass prairie: Biophysical and physical controls. In: *Stable Isotopes and Biosphere–Atmosphere Interactions*, Physiological Ecology Series (eds Flanagan LB, Ehleringer JR, Pataki D), Elsevier, Academic Press, Amsterdam, in press.

Suyker AE, Verma SB (2001) Year-round observations of the net ecosystem exchange of carbon dioxide in a native tallgrass prairie. *Global Change Biology*, **7**, 279–289.

Tans PP (1980) On calculating the transfer of ^{13}C in reservoir models of the carbon cycle. *Tellus*, **32**, 464–469.

Tans PP (1998) Oxygen isotopic equilibrium between carbon dioxide and water in soils. *Tellus Series B-Chemical and Physical Meteorology*, **50**, 163–178.

Wang XF, Yakir D (2000) Using stable isotopes of water in evapotranspiration studies. *Hydrological Processes*, **14**, 1407–1421.

Yakir D, Sternberg LDL (2000) The use of stable isotopes to study ecosystem gas exchange. *Oecologia*, **123**, 297–311.

Yakir D, Wang X-F (1996) Fluxes of CO$_2$ and water between terrestrial vegetation and the atmosphere estimated from isotope measurements. *Nature*, **381**, 515–518.